*Journal of the European Ceramic Society* **10** (1992) 415–424

# Interfacial Phenomena in $Al_2O_3$–Liquid Metal and $Al_2O_3$–Liquid Alloy Systems

P. Nikolopoulos

University of Patras, Chemical Engineering Department, Materials Science and Technology Section, GR-261 10 Patras, Greece

&

S. Agathopoulos

Institute of Chemical Engineering and High Temperature Chemical Processes, PO Box 1239, GR-261 10 Patras, Greece

(Received 7 August 1991; accepted 5 November 1991)

***Abstract***

*The sessile drop technique has been used to measure the contact angle of liquid metals and liquid alloys in contact with polycrystalline alumina. The experiments were carried out in argon atmosphere at various temperatures. The measured contact angles exhibit no wettability ($\theta > 90°$). The linear temperature functions of the work of adhesion as well as of the interfacial energy were also determined in the investigated systems. The partial high values of the work of adhesion in several $Al_2O_3$–liquid metal systems can be attributed to a chemical bond establishment at the interface. The values of the interfacial energies at the melting point of the metals, for non-reactive $Al_2O_3$–liquid metal systems, vary in a restricted region ($2{\cdot}35$–$2{\cdot}75\ J\,m^{-2}$). An empirical relation is proposed for evaluation of the interfacial energy of the metals at their melting point. The agreement between experimental and calculated values is satisfactory.*

*Mit Hilfe der Methode des 'Liegenden Tropfens' wurde der Benetzungswinkel von geschmolzenen Metallen bzw. Legierungen in Kontakt mit polykristallinem Aluminium oxid bestimmt. Die Experimente wurden in Argonatmosphäre bei verschiedenen Temperaturen durchgeführt. Die gemessenen Winkelwerte zeigen, dass keine Benetzung stattfindet ($\theta > 90°$). In den untersuchten Systemen wurden die linearen Temperaturfunktionen sowohl der Adhäsionsarbeit als auch der Grenzflächenenergie bestimmt. Die zum Teil hohen Werte der Adhäsionsarbeit in einigen Systemen von $Al_2O_3$-Metallschmelzen können mit der Anwesenheit von chemischen Bindungen an der Grenzfläche erklärt werden. Die Werte der Grenzflächenenergien am Schmelzpunkt der Metalle, für nicht-reagierende Systeme von $Al_2O_3$ Metallschmelzen, variieren in einem begrenzten Bereich ($2{\cdot}35$–$2{\cdot}75\ J\,m^{-2}$). Im weiteren wird eine empirische Beziehung zur Abschätzung der Grenzflächenenergie der Metalle an ihren Schmelzpunkten vorgestellt. Die Übereinstimmung zwischen experimentell bestimmten und errechneten Werten ist zufriedenstellend.*

*La méthode des gouttelettes sessiles a été utilisée pour mesurer l'angle de contact entre métaux et alliages liquides avec de l'alumine polycristalline. Les expériences ont été effectuées sous atmosphère d'argon à différentes températures. Les angles de contact mesurés ne montrent pas de mouillabilité ($\theta > 90°$). Les fonctions linéaires en température du travail d'adhésion ainsi que de l'énergie d'interface ont aussi été déterminées pour les systèmes étudiés. Les valeurs partiellement élevées du travail d'adhésion pour plusieurs systèmes $Al_2O_3$–métal liquide peuvent être attribuées à l'établissement du liaison chimique à l'interface. Les valeurs des énergies d'interfaces au point de fusion des métaux, pour des systémes $Al_2O_3$–métal liquide non réactifs chimiquement, varient dans un domaine réduit ($2{\cdot}35$–$2{\cdot}75\ J\,m^{-2}$). Une relation empirique est proposée pour évaluer l'énergie d'inter-*



*Journal of the European Ceramic Society* 0955-2219/92/$5.00 

*face des métaux à leur point de fusion. La correspondance entre les valeurs expérimentales et les valeurs calculées est satisfaisante.*

## 1 Introduction

The interfacial properties between ceramics and metals are of importance in the development of joining techniques as well as in problems related to powder technology consolidation of two-phase or multiphase materials. With regard to the commercial viability of engineering ceramics,[1] techniques are required for the joining of ceramics to metallic components. Brazing, diffusion welding and processes in which one of the two work pieces involved is fused are suitable for application in the high-temperature range, which is of particular interest.[2] On the other hand, when a liquid is present during sintering of a ceramic–metal powder composite material (cermet), the density, microstructure and mechanical properties of the cermet are influenced by the wetting behavior at the interface.

The correlation between the wetting and the bonding behavior at the interface in solid–liquid–vapor systems in thermodynamic equilibrium is given by eqn (1):

$$W_a = \gamma_{SV} + \gamma_{LV} - \gamma_{SL} \quad (1)$$

where $\gamma_{SV}$ and $\gamma_{LV}$ are the surface energies of the solid and the liquid phase, respectively, $\gamma_{SL}$ is the interfacial energy of solid–liquid, and $W_a$ is the work of adhesion, defined as the work needed to separate the interface.

An established method for studying the interfacial phenomena is that of a sessile drop of liquid metal lying on a solid ceramic substrate (Fig. 1). In this case the following equation holds:

$$\gamma_{SL} = \gamma_{SV} - \gamma_{LV} \cos\theta \quad (2)$$

where $\theta$ is the contact angle.

Introduction of eqn (1) into eqn (2) gives

$$W_a = \gamma_{LV}(1 + \cos\theta) \quad (3)$$

Using eqns (2) and (3), experimental data of the contact angle $\theta$ and values of $\gamma_{SV}$ and $\gamma_{LV}$ from the literature, the quantities of $\gamma_{SL}$ and $W_a$ can be calculated.

The present work concerns the experimental and theoretical treatments that have been carried out in order to determine the works of adhesion and the interfacial energies and their temperature functions in $Al_2O_3$–liquid metal (In, Ag, Ni, Fe, Pd) systems as well as in $Al_2O_3$–liquid alloy (Bi–Pb, Bi–Sn, Sn–Pb, Bi–Pb–Sn, Cu–Sn, Cu–Ni) systems. Additional literature data about contact angles under the same conditions, i.e. apparatus, atmosphere and substrate, in ($Al_2O_3$–Sn, –Co)[3] and ($Al_2O_3$–Bi, –Pb, –Cu),[4] supplement the experimentally determined values.

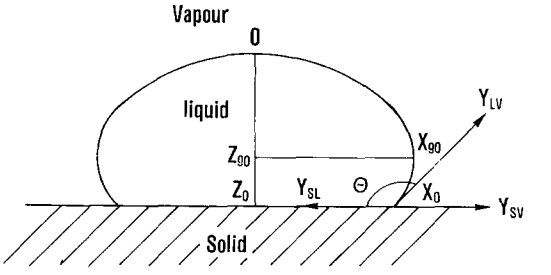


**Fig. 1.** Contact angle ($\theta$) in solid–liquid–vapor system in equilibrium.

## 2 Wetting Experiments (Procedure and Results)

Polished disks (20 mm diameter, 3 mm thickness) of polycrystalline alumina Al23 (Friedrichsfeld Co., FRG) with purity of >99·5% wt% was used as solid substrate in wetting experiments. The as-received $Al_2O_3$ had a density of 3·7–3·95 Mg m$^{-3}$, a grain size of 10–20 $\mu$m and no open porosity. According to the chemical analysis given by the manufacturer, the alumina also contained (in wt%): $SiO_2$, 0·05–0·1; MgO, 0·2; CaO, 0·05; $Fe_2O_3$, 0·02–0·05; $Na_2O$, 0·1–0·3.

The metals In, Ag, Ni, Fe, Pd and the eutectic alloys Bi–Pb (55·5/44·5), Bi–Sn (58/42), Sn–Pb (61·9/38·1) and Bi–Pb–Sn (52·5/32/15·5) as well as the copper alloys Cu–Sn (90/10) and Cu–Ni (74·5/25·5) (Ventron GmbH, FRG) of high purity and low oxygen concentration (≤0·003 wt%) were used (the values in parentheses represent the wt% concentration of the alloys). Low oxygen concentrations are needed because oxygen is a surface active element that suppresses[5] the surface energies of the liquid metals and alloys as well as the interfacial energies between them and ceramics when it is present at higher concentrations.

The measurements were carried out in a purified argon atmosphere. The samples were heated by an induction furnace.[6] Contact angles were measured from photographs of the sessile drop. The temperature was measured with a thermocouple as well as by optical pyrometry with an accuracy of ±10 K. For a given system and temperature, two to four experiments were carried out. Each experiment lasted for 20–30 min. Photographs of the sessile drop were obtained at 5-min intervals.

Owing to the fact that the contact angle, $\theta$, in all

systems examined was greater than 90°, the sessile drop has the form of an ellipsoid of revolution. From the values $X_{90}$, $Z_{90}$, $X_0$ and $Z_0$ (Fig. 1), and by using the tables of Bashford & Adams,[7] the contact angle can be determined. Meanwhile, previous works have proved that the influence of metal vapors, existing in the furnace atmosphere, has a negligible effect on the surface energy of ceramics and therefore on the values of contact angles, so it has been neglected.[3,8] Experimental results show that contact angle is time independent in all systems examined.

Figures 2 and 3 show the temperature dependence of the contact angle in the systems $Al_2O_3$–In, –Sn, –Bi, –Pb, –Ag, –Cu, –Ni, –Co, –Fe and –Pd (Fig. 2) and in the systems $Al_2O_3$–(Bi–Pb), –(Bi–Sn), –(Sn–Pb), –(Bi–Pb–Sn), –(Cu–Sn) and –(Cu–Ni) (Fig. 3), respectively.

The values of the measured contact angles agree reasonably well with most of the literature data obtained under inert gas or vacuum conditions for $Al_2O_3$–liquid metals[9–11] and $Al_2O_3$–liquid alloys.[12] Results indicate that liquid metals and alloys, within the investigated temperature range, do not wet the alumina ceramic, i.e. $\gamma_{SL} > \gamma_{SV}$ (eqn (2)). This is frequently attributed to the domination of oxygen anions on the ceramic surface. The contact angle decreases with increasing temperature. In general, the contact angle decreases with the increasing melting point of the metal (Fig. 2). Therefore, better wettability is shown in the case of high melting point metals in contact with alumina. Experimental results with alloys (Fig. 3) indicate that the wettability is not considerably improved compared to that of the pure metals.

Moreover, the values of contact angle indicate that the wettability is not sufficient for high densification of composites during liquid-phase

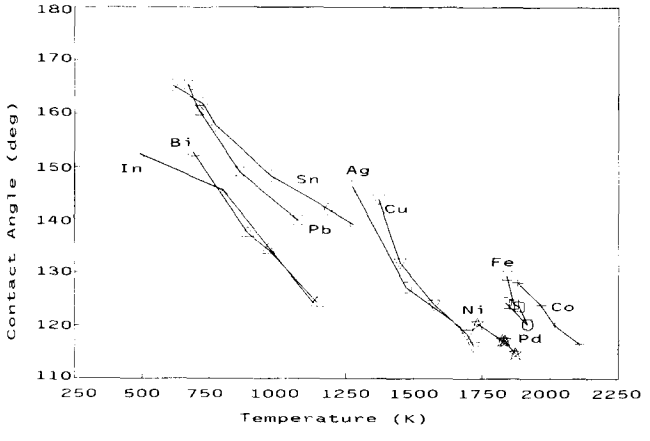


**Fig. 2.** Effect of temperature on the contact angles formed by liquid metals on $Al_2O_3$.

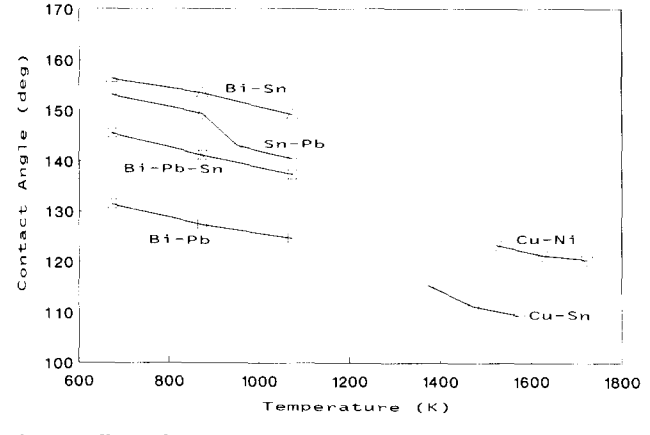


**Fig. 3.** Effect of temperature on the contact angles formed by liquid alloys on $Al_2O_3$.

**Table 1.** Contact angles ($\theta$) in $Al_2O_3$–liquid metal systems

| *System* | *T (K)* | *Contact angle (deg)* |
|---|---|---|
| $Al_2O_3$–In | 493 | 152·35 ± 4·59 |
| | 798 | 145·63 ± 5·01 |
| | 1 128 | 124·29 ± 4·98 |
| $Al_2O_3$–Sn[3] | 611 | 165·24 ± 4·06 |
| | 726 | 161·74 ± 2·68 |
| | 772 | 157·74 ± 7·86 |
| | 975 | 148·26 ± 4·37 |
| | 1 183 | 141·96 ± 1·71 |
| | 1 280 | 138·95 ± 2·67 |
| $Al_2O_3$–Bi[4] | 689 | 152·73 ± 4·95 |
| | 890 | 137·38 ± 2·99 |
| | 965 | 134·33 ± 1·90 |
| | 1 144 | 125·24 ± 1·86 |
| $Al_2O_3$–Pb[4] | 667 | 165·30 ± 3·05 |
| | 711 | 160·48 ± 7·15 |
| | 860 | 149·00 ± 5·18 |
| | 1 073 | 139·82 ± 10·05 |
| $Al_2O_3$–Ag | 1 273 | 146·22 ± 3·62 |
| | 1 473 | 127·19 ± 1·01 |
| | 1 673 | 119·67 ± 2·58 |
| $Al_2O_3$–Cu[4] | 1 370 | 143·87 ± 2·82 |
| | 1 450 | 131·86 ± 2·66 |
| | 1 575 | 123·97 ± 2·30 |
| | 1 695 | 118·42 ± 1·42 |
| | 1 720 | 116·10 ± 1·19 |
| $Al_2O_3$–Ni | 1 733 | 120·36 ± 1·12 |
| | 1 823 | 117·25 ± 1·10 |
| | 1 833 | 117·13 ± 1·13 |
| | 1 873 | 114·72 ± 1·57 |
| $Al_2O_3$–Co[3] | 1 888 | 128·20 ± 2·81 |
| | 1 973 | 123·91 ± 2·12 |
| | 2 023 | 120·10 ± 1·53 |
| | 2 113 | 116·68 ± 0·88 |
| $Al_2O_3$–Fe | 1 848 | 129·46 ± 1·00 |
| | 1 873 | 124·08 ± 0·52 |
| | 1 893 | 123·62 ± 1·21 |
| | 1 923 | 120·38 ± 5·04 |
| $Al_2O_3$–Pd | 1 853 | 124·37 ± 0·89 |
| | 1 913 | 119·96 ± 0·74 |

**Table 2.** Contact angles ($\theta$) in $Al_2O_3$–liquid alloy systems

| *System* | *T (K)* | *Contact angle (deg)* |
|---|---|---|
| $Al_2O_3$–Bi–Pb | 673 | 131·40 ± 3·42 |
| | 873 | 127·47 ± 1·66 |
| | 1 073 | 124·76 ± 0·87 |
| $Al_2O_3$–Bi–Sn | 673 | 156·32 ± 1·81 |
| | 873 | 153·56 ± 2·94 |
| | 1 073 | 149·26 ± 4·10 |
| $Al_2O_3$–Sn–Pb | 673 | 153·14 ± 2·03 |
| | 873 | 149·52 ± 4·65 |
| | 951 | 143·04 ± 11·51 |
| | 1 073 | 140·49 ± 13·70 |
| $Al_2O_3$–Bi–Pb–Sn | 673 | 145·56 ± 3·03 |
| | 873 | 141·25 ± 1·36 |
| | 1 073 | 137·36 ± 0·64 |
| $Al_2O_3$–Cu–Sn | 1 373 | 115·42 ± 2·75 |
| | 1 473 | 111·21 ± 5·43 |
| | 1 573 | 109·36 ± 1·89 |
| $Al_2O_3$–Cu–Ni | 1 523 | 123·32 ± 4·06 |
| | 1 623 | 121·32 ± 1·75 |
| | 1 723 | 120·42 ± 2·47 |

sintering as well as for the joining of ceramics to metallic components.

After each wetting experiment, removal of the solid drop from the ceramic surface (by pushing the drop) was attempted. No adherence was observed at the interface between ceramic and the metals or alloys, except in the $Al_2O_3$–Ni system, where a strong force was needed to remove the nickel drop from some of the solid substrates. Metallographic observation showed irregularities at the alumina–nickel interface. However, it has been shown that the presence of elevated oxygen concentration at the interface gives rise to the formation of a spinel interface.[13]

The measured values of contact angle for the systems of $Al_2O_3$–liquid metals and $Al_2O_3$–liquid alloys, together with literature data, are summarized in Tables 1 and 2, respectively.

## 3 Work of Adhesion

The values of work of adhesion, $W_a$, follow the expression

$$0 \leq W_a \leq 2\gamma_{LV} = W_c$$

where $W_c$ is the work of cohesion. The work of adhesion is calculated by eqn (3), using the experimental values of contact angle and the surface energy of the liquid metallic phase. In the case of liquid metals, surface energies are directly calculated using literature data. Table 3 shows the linear temperature functions of liquid metals (In, Ag, Cu),[14] (Sn, Pb, Pd),[15] Bi[16] and (Ni, Co, Fe).[14,17]

The surface energies of liquid binary (or ternary) alloys are calculated using the equation for ideal mixtures of Belton & Evans:[18]

$$\gamma_{LV,M} = \gamma_{LV,i} + \frac{RT}{A_i} \ln \frac{x_i'}{x_i} \tag{4}$$

where $\gamma_{LV,M}$ and $\gamma_{LV,i}$ are the surface energies of the mixture and its components, respectively, $x_i$ and $x_i'$ are the mole fractions in the bulk and at the surface layer, respectively, and $A_i$ the molar surface area of the components. Equation (4) is valid under the assumptions that (a) the surface phase is considered as monolayer and (b) the molar surface areas of the components are equal.

Guggenheim[19] uses the method of the grand partition function, and obtained the symmetrical form derived from eqn (4):

$$\exp\left(-\frac{\gamma_{LV,M}A}{RT}\right) = \sum_i x_i \exp\left(-\frac{\gamma_{LV,i}A}{RT}\right) \tag{5}$$

For the calculations, the molar surface area, $A$, is given as the mean molar surface area of the components ($A_i$). The $A_i$ value is obtained using eqn (6):

$$A_i = 1{\cdot}091 N_0^{1/3} \left(\frac{M_i}{\rho_{L,i}}\right)^{2/3} \tag{6}$$

**Table 3.** Linear temperature functions of the surface energies ($\gamma_{LV}$) of liquid metals

| *Metal* | *Surface energy* ($Jm^{-2}$) | *Temperature* (*K*) | *Reference* |
|---|---|---|---|
| In | $0{\cdot}560 - 0{\cdot}09 \times 10^{-3}(T - T_m)$ | $T \geq T_m = 429$ | 14 |
| Sn | $0{\cdot}544 - 0{\cdot}07 \times 10^{-3}(T - T_m)$ | $T \geq T_m = 505$ | 15 |
| Bi | $0{\cdot}372 - 0{\cdot}09 \times 10^{-3}(T - T_m)$ | $T \geq T_m = 544$ | 16 |
| Pb | $0{\cdot}468 - 0{\cdot}13 \times 10^{-3}(T - T_m)$ | $T \geq T_m = 600$ | 15 |
| Ag | $0{\cdot}912 - 0{\cdot}15 \times 10^{-3}(T - T_m)$ | $T \geq T_m = 1\,234$ | 14 |
| Cu | $1{\cdot}311 - 0{\cdot}20 \times 10^{-3}(T - T_m)$ | $T \geq T_m = 1\,356$ | 14 |
| Ni | $1{\cdot}754 - 0{\cdot}28 \times 10^{-3}(T - T_m)$ | $T \geq T_m = 1\,726$ | 14, 17 |
| Co | $1{\cdot}831 - 0{\cdot}29 \times 10^{-3}(T - T_m)$ | $T \geq T_m = 1\,768$ | 14, 17 |
| Fe | $1{\cdot}825 - 0{\cdot}27 \times 10^{-3}(T - T_m)$ | $T \geq T_m = 1\,809$ | 14, 17 |
| Pd | $1{\cdot}500 - 0{\cdot}22 \times 10^{-3}(T - T_m)$ | $T \geq T_m = 1\,825$ | 15 |

**Table 4.** Linear temperature functions of the surface energies ($\gamma_{LV}$) of liquid alloys

| *Alloy composition* (*wt%*) | *Surface energy* ($J m^{-2}$) | *Temperature* (*K*) |
|---|---|---|
| Bi–Pb (55·5/44·5) | $0{\cdot}415 - 0{\cdot}09 \times 10^{-3}(T - T_m)$ | $T \geq T_m = 397$ (eutectic) |
| Bi–Sn (58/42) | $0{\cdot}430 - 0{\cdot}05 \times 10^{-3}(T - T_m)$ | $T \geq T_m = 412$ (eutectic) |
| Sn–Pb (61·9/38·1) | $0{\cdot}525 - 0{\cdot}09 \times 10^{-3}(T - T_m)$ | $T \geq T_m = 456$ (eutectic) |
| Bi–Pb–Sn (52·5/32/15·5) | $0{\cdot}427 - 0{\cdot}07 \times 10^{-3}(T - T_m)$ | $T \geq T_m = 368$ (eutectic) |
| Cu–Sn (90/10) | $1{\cdot}232 - 0{\cdot}17 \times 10^{-3}(T - T_m)$ | $T \geq 1\,270$ |
| Cu–Ni (74·5/25·5) | $1{\cdot}363 - 0{\cdot}19 \times 10^{-3}(T - T_m)$ | $T \geq 1\,520$ |

where $N_0$ is the Avogadro number, $M_i$ the molecular weight of the metal and $\rho_{L,i}$ the density of the liquid metal. The temperature dependence of $\rho_{L,i}$ is given by Allen.[15]

Table 4 shows the linear temperature functions of liquid alloys Bi–Pb, Bi–Sn, Sn–Pb, Bi–Pb–Sn, Cu–Sn and Cu–Ni, which were calculated using eqn (5). Comparison between values calculated using equations of Table 4 and literature data for Sn–Pb at 623 K[20] and 823 K,[20,21] Cu–Sn at 1423 K[22] and Cu–Ni at 1773 K[23] seems in good accordance.

**Table 5.** Work of adhesion ($W_a$) and linear temperature functions of $W_a$ in $Al_2O_3$–liquid metal systems ($R$ = correlation coefficient)

| *System* | $T$ (*K*) | $W_a$ ($J m^{-2}$) | $W_a(T) = W_{a,T_m} + \frac{dW_a}{dT}(T - T_M)$ ($J m^{-2}$) |
|---|---|---|---|
| $Al_2O_3$–In | 493 | 0·062 | $0{\cdot}031 + 0{\cdot}246 \times 10^{-3}(T - 429)$ |
| | 798 | 0·092 | $R = 0{\cdot}950\,055$ |
| | 1 128 | 0·217 | |
| $Al_2O_3$–Sn | 611 | 0·018 | $-0{\cdot}003 + 0{\cdot}160 \times 10^{-3}(T - 505)$ |
| | 726 | 0·027 | $R = 0{\cdot}996\,664$ |
| | 772 | 0·039 | |
| | 975 | 0·076 | |
| | 1 183 | 0·106 | |
| | 1 280 | 0·120 | |
| $Al_2O_3$–Bi | 689 | 0·040 | $0{\cdot}013 + 0{\cdot}208 \times 10^{-3}(T - 544)$ |
| | 890 | 0·090 | $R = 0{\cdot}995\,324$ |
| | 965 | 0·101 | |
| | 1 144 | 0·135 | |
| $Al_2O_3$–Pb | 667 | 0·015 | $0{\cdot}004 + 0{\cdot}200 \times 10^{-3}(T - 600)$ |
| | 711 | 0·026 | $R = 0{\cdot}994\,024$ |
| | 860 | 0·062 | |
| | 1 073 | 0·096 | |
| $Al_2O_3$–Ag | 1 273 | 0·153 | $0{\cdot}145 + 0{\cdot}685 \times 10^{-3}(T - 1234)$ |
| | 1 473 | 0·346 | $R = 0{\cdot}973\,264$ |
| | 1 673 | 0·427 | |
| $Al_2O_3$–Cu | 1 370 | 0·252 | $0{\cdot}278 + 1{\cdot}158 \times 10^{-3}(T - 1356)$ |
| | 1 450 | 0·430 | $R = 0{\cdot}981\,071$ |
| | 1 575 | 0·559 | |
| | 1 695 | 0·651 | |
| | 1 720 | 0·693 | |
| $Al_2O_3$–Ni | 1 733 | 0·866 | $0{\cdot}855 + 0{\cdot}889 \times 10^{-3}(T - 1726)$ |
| | 1 823 | 0·936 | $R = 0{\cdot}980\,960$ |
| | 1 833 | 0·938 | |
| | 1 873 | 0·997 | |
| $Al_2O_3$–Co | 1 888 | 0·685 | $0{\cdot}541 + 1{\cdot}226 \times 10^{-3}(T - 1768)$ |
| | 1 973 | 0·783 | $R = 0{\cdot}991\,385$ |
| | 2 023 | 0·876 | |
| | 2 113 | 0·954 | |
| $Al_2O_3$–Fe | 1 848 | 0·661 | $0{\cdot}575 + 2{\cdot}816 \times 10^{-3}(T - 1809)$ |
| | 1 873 | 0·795 | $R = 0{\cdot}955\,389$ |
| | 1 893 | 0·804 | |
| | 1 923 | 0·887 | |
| $Al_2O_3$–Pd | 1 853 | 0·651 | $0{\cdot}609 + 1{\cdot}500 \times 10^{-3}(T - 1825)$ |
| | 1 913 | 0·741 | |

The calculated values of work of adhesion in $Al_2O_3$–liquid metal and alloy systems are listed in Tables 5 and 6, respectively. Correlation of $W_a$ values with corresponding temperature values indicates that the work of adhesion can be described sufficiently by linear temperature functions for each ceramic–metal or –alloy system. These functions with their correlation coefficients, $R$, are also included in Tables 5 and 6. In all cases the temperature coefficients of $W_a$, $dW_a/dT$, are positive.

The temperature dependence of $W_a$ in $Al_2O_3$–liquid metal and alloy systems is presented in Figs 4 and 5. Linear extrapolation of $W_a$ to the melting point of the metals, $W_{a,T_m}$, indicates that metals with high melting point and high surface energy have higher values of work of adhesion and temperature

**Table 6.** Work of adhesion ($W_a$) and linear temperature functions of $W_a$ in $Al_2O_3$–liquid alloy systems ($R$ = correlation coefficient)

| *System* | $T$ (*K*) | $W_a$ ($J m^{-2}$) | $W_a(T) = W_{a,T_m} + \frac{dW_a}{dT}(T - T_M)$ ($J m^{-2}$) |
|---|---|---|---|
| $Al_2O_3$–Bi–Pb | 673 | 0·132 | $0{\cdot}120 + 0{\cdot}050 \times 10^{-3}(T - 397)$ |
| | 873 | 0·146 | $R = 0{\cdot}974\,355$ |
| | 1 073 | 0·152 | |
| $Al_2O_3$–Bi–Sn | 673 | 0·035 | $0{\cdot}020 + 0{\cdot}053 \times 10^{-3}(T - 412)$ |
| | 873 | 0·043 | $R = 0{\cdot}990\,684$ |
| | 1 073 | 0·056 | |
| $Al_2O_3$–Sn–Pb | 673 | 0·054 | $0{\cdot}020 + 0{\cdot}139 \times 10^{-3}(T - 456)$ |
| | 873 | 0·067 | $R = 0{\cdot}947\,187$ |
| | 951 | 0·096 | |
| | 1 073 | 0·107 | |
| $Al_2O_3$–Bi–Pb–Sn | 673 | 0·071 | $0{\cdot}049 + 0{\cdot}072 \times 10^{-3}(T - 368)$ |
| | 873 | 0·086 | $R = 0{\cdot}999\,802$ |
| | 1 073 | 0·100 | |
| $Al_2O_3$–Cu–Sn | 1 373 | 0·693 | $0{\cdot}651 + 0{\cdot}480 \times 10^{-3}(T - 1270)$ |
| | 1 473 | 0·764 | $R = 0{\cdot}963\,798$ |
| | 1 573 | 0·789 | |
| $Al_2O_3$–Cu–Ni | 1 523 | 0·614 | $0{\cdot}617 + 0{\cdot}200 \times 10^{-3}(T - 1520)$ |
| | 1 623 | 0·645 | $R = 0{\cdot}953\,102$ |
| | 1 723 | 0·654 | |

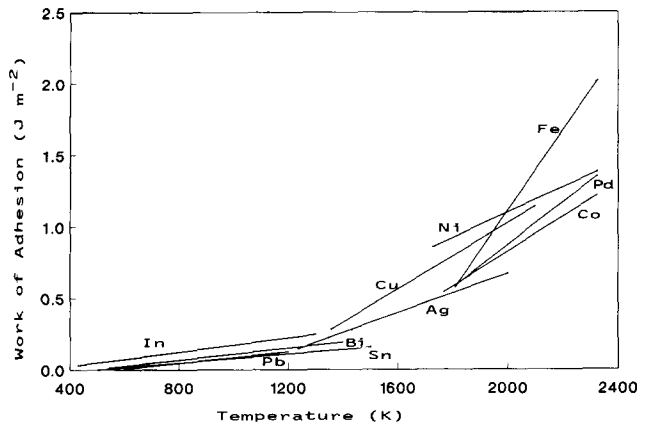


**Fig. 4.** Work of adhesion ($W_a$)—temperature dependence in $Al_2O_3$–liquid metal systems.

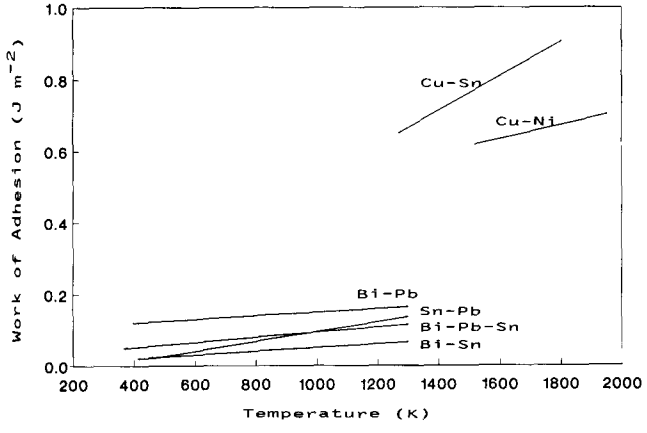


**Fig. 5.** Work of adhesion ($W_a$)—temperature dependence in $Al_2O_3$–liquid alloy systems.

coefficients. This result can be taken as an indication that in the case of high melting point metals, despite the effect of non-wetting phenomena, an interface may be formed which positively influences the mechanical properties of the ceramic–metal composite material.

The values of $W_{a,T_m}$ obtained from diverse systems are dispersed from $\simeq 0$ to 0·85 J m$^{-2}$. This dispersion depends on the metal and can be explained if the forces that play a role at the ceramic–metal interface are taken into account.

The work of adhesion between two phases, in the general case, can be presented in the form[11]

$$W_a = W_a(\text{equil.}) + W_a(\text{non-equil.}) \quad (7)$$

The magnitude of $W_a$(non-equil.) represents the amount of energy released when a reaction takes place at the interface. The magnitude of $W_a$(equil.) corresponds to non-reactive systems and can be divided in two separate terms:

$$W_a(\text{equil.}) = W_a(\text{chem.equil.}) + W_a(\text{VDW}) \quad (8)$$

where $W_a$(chem. equil.) is the cohesive energy between solid and liquid phases due to establishment of chemical equilibrium bonds by mutual saturation of the free valences of the surfaces in contact, and $W_a$(VDW) represents the energy of van der Waals (VDW) interactions (dispersion forces).

Neglecting the non-equilibrium contribution of work of adhesion in the systems with a positive value of the Gibbs free energy of reaction between the liquid metal and the oxide, the calculated $W_a$(VDW) values[11] have an upper limit of about 0·5 J m$^{-2}$. Consequently, a high deviation between $W_a$(VDW) and experimental values of $W_a$ is presented, especially in high melting point metals.

Chatain *et al.*[9] developed a model considering that interactions at the interface of non-reactive ceramic–metal systems are essentially chemical. According to this model, two kinds of chemical bonds are established. One between the liquid metal, Me, and the oxygen ion, $O^{2-}$, of the oxide, and the other one between the liquid metal, Me, and the metal of the oxide, M. The application of this model to $Al_2O_3$–liquid metal systems agrees well with the experimental data,[9] assuming that the work of adhesion in all systems examined is a weak function of the temperature, so a mean value for each system satisfactorily represents the experimental results.

In general, the interactions at the ceramic–liquid metal interface, in non-reactive systems, can take place by physical van der Waals forces only, and in the case of transition metals also by establishing a chemical bond.[24]

## 4 Interfacial Energy

In order to determine interfacial energies, $\gamma_{SL}$, in $Al_2O_3$–liquid metal and alloy systems (eqn (2)), apart from the data available on contact angles, $\theta$ (Tables 1 and 2), and the surface energies of liquids, $\gamma_{LV}$ (Tables 3 and 4), it is necessary to know the magnitude of the surface energy of $Al_2O_3$, whose dependence of the temperature is given as[3]

$$\gamma_{SV}(Al_2O_3) = 2{\cdot}559 - 0{\cdot}784 \times 10^{-3}T \quad (\text{J m}^{-2}) \quad (9)$$

According to eqn (2), the calculated values of interfacial energies in $Al_2O_3$–liquid metal and $Al_2O_3$–liquid alloy systems, together with their linear temperature functions, are included in Tables 7 and 8, respectively. The $\gamma_{SL}$ values indicate that, in general, the interfacial energy at the melting point of both metals and alloys, $\gamma_{SL,T_m}$, decreases when the melting point increases. Furthermore, no appreciable deviation is observed between the interfacial energies of the metals and the alloys of these metals.

**Table 7.** Interfacial energy ($\gamma_{SL}$) and linear temperature functions of $\gamma_{SL}$ in $Al_2O_3$–liquid metal systems ($R$ = correlation coefficient)

| *System* | $T$ ($K$) | $\gamma_{SL}$ ($Jm^{-2}$) | $\gamma_{SL}(T)=\gamma_{SL,T_m}+\frac{d\gamma_{SL}}{dT}(T-T_M)$ ($Jm^{-2}$) |
|---|---|---|---|
| $Al_2O_3$–In | 493 | 2·663 | $2·750-1·117\times10^{-3}(T-429)$ |
| | 798 | 2·368 | $R=0·997\,322$ |
| | 1 128 | 1·955 | |
| $Al_2O_3$–Sn | 611 | 2·599 | $2·710-1·014\times10^{-3}(T-505)$ |
| | 726 | 2·492 | $R=0·999\,915$ |
| | 772 | 2·440 | |
| | 975 | 2·230 | |
| | 1 183 | 2·023 | |
| | 1 280 | 1·925 | |
| $Al_2O_3$–Bi | 689 | 2·338 | $2·492-1·083\times10^{-3}(T-544)$ |
| | 890 | 2·112 | $R=0·999\,816$ |
| | 965 | 2·035 | |
| | 1 144 | 1·845 | |
| $Al_2O_3$–Pb | 667 | 2·480 | $2·552-1·112\times10^{-3}(T-600)$ |
| | 711 | 2·430 | $R=0·999\,793$ |
| | 860 | 2·257 | |
| | 1 073 | 2·029 | |
| $Al_2O_3$–Ag | 1 273 | 2·314 | $2·359-1·620\times10^{-3}(T-1234)$ |
| | 1 473 | 1·934 | $R=0·995\,058$ |
| | 1 673 | 1·666 | |
| $Al_2O_3$–Cu | 1 370 | 2·541 | $2·528-2·141\times10^{-3}(T-1356)$ |
| | 1 450 | 2·284 | $R=0·994\,308$ |
| | 1 575 | 2·032 | |
| | 1 695 | 1·822 | |
| | 1 720 | 1·756 | |
| $Al_2O_3$–Ni | 1 733 | 2·086 | $2·105-1·947\times10^{-3}(T-1726)$ |
| | 1 823 | 1·921 | $R=0·996\,000$ |
| | 1 833 | 1·908 | |
| | 1 873 | 1·807 | |
| $Al_2O_3$–Co | 1 888 | 2·190 | $2·463-2·301\times10^{-3}(T-1768)$ |
| | 1 973 | 2·001 | $R=0·997\,537$ |
| | 2 023 | 1·854 | |
| | 2 113 | 1·679 | |
| $Al_2O_3$–Fe | 1 848 | 2·263 | $2·391-3·873\times10^{-3}(T-1809)$ |
| | 1 873 | 2·104 | $R=0·976\,680$ |
| | 1 893 | 2·073 | |
| | 1 923 | 1·958 | |
| $Al_2O_3$–Pd | 1 853 | 1·949 | $2·019-2·500\times10^{-3}(T-1825)$ |
| | 1 913 | 1·799 | |

**Table 8.** Interfacial energy ($\gamma_{SL}$) and linear temperature functions of $\gamma_{SL}$ in $Al_2O_3$–liquid alloy systems ($R$ = correlation coefficient)

| *System* | $T$ ($K$) | $\gamma_{SL}$ ($Jm^{-2}$) | $\gamma_{SL}(T)=\gamma_{SL,T_m}+\frac{d\gamma_{SL}}{dT}(T-T_M)$ ($Jm^{-2}$) |
|---|---|---|---|
| $Al_2O_3$–Bi–Pb | 673 | 2·289 | $2·542-0·922\times10^{-3}(T-397)$ |
| | 873 | 2·101 | $R=0·999\,940$ |
| | 1 073 | 1·920 | |
| $Al_2O_3$–Bi–Sn | 673 | 2·413 | $2·645-0·885\times10^{-3}(T-412)$ |
| | 873 | 2·239 | $R=0·999\,952$ |
| | 1 073 | 2·059 | |
| $Al_2O_3$–Sn–Pb | 673 | 2·482 | $2·705-1·012\times10^{-3}(T-456)$ |
| | 873 | 2·295 | $R=0·998\,815$ |
| | 951 | 2·197 | |
| | 1 073 | 2·080 | |
| $Al_2O_3$–Bi–Pb–Sn | 673 | 2·366 | $2·648-0·925\times10^{-3}(T-368)$ |
| | 873 | 2·181 | $R=1·000\,000$ |
| | 1 073 | 1·996 | |
| $Al_2O_3$–Cu–Sn | 1 373 | 2·004 | $2·144-1·435\times10^{-3}(T-1270)$ |
| | 1 473 | 1·837 | $R=0·995\,560$ |
| | 1 573 | 1·717 | |
| $Al_2O_3$–Cu–Ni | 1 523 | 2·113 | $2·113-1·175\times10^{-3}(T-1520)$ |
| | 1 623 | 1·985 | $R=0·998\,672$ |
| | 1 723 | 1·878 | |

The negative slope of the linear temperature functions of the interfacial energies, $d\gamma_{SL}/dT$, shows that wettability is improved when temperature increases in all systems. The absolute values of the slope increase with increase of the melting point of the metal. This means that at temperatures far enough from the melting point of the metals a high adherence between a high melting point metal and the ceramic substrate would be expected.

The values of the interfacial energies in $Al_2O_3$–liquid metal systems at the melting point of the metals are substantially higher than those in the systems of the same metals in contact with cubic oxides of $UO_2$[8] and $ZrO_2$.[25] This result points out a weaker bonding behavior in $Al_2O_3$–liquid metal interfaces than the interfaces in the case of $UO_2$ and $ZrO_2$.

Figures 6 and 7 show the linear temperature functions of the interfacial energies of the $Al_2O_3$–liquid metal and alloy systems, respectively. The temperature function of the surface energy of $Al_2O_3$, $\gamma_{SV}$, is represented with a dashed line. The lines for the interfacial energies in Fig. 6 begin at the melting point of the metals and are extrapolated up to the corresponding boiling point. In the case where the boiling point is higher than the melting point of alumina ($T_m = 2323$ K), then the lines are extrapolated to the melting point of aluminum oxide. The linear function of the surface energy of alumina

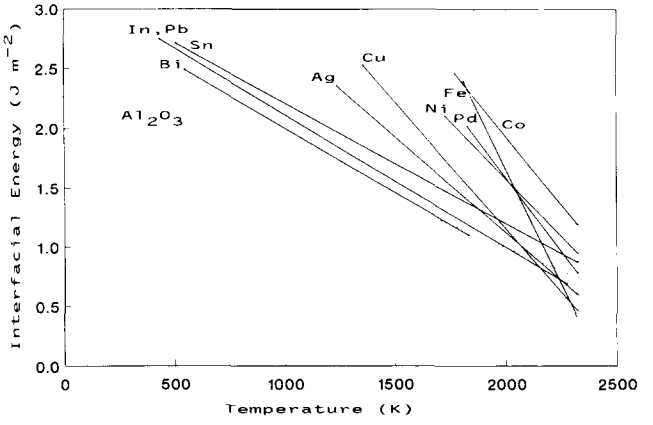


**Fig. 6.** Temperature dependence of the surface energy ($\gamma_{SV}$) of $Al_2O_3$ (– – –) and of the interfacial energy ($\gamma_{SL}$) in $Al_2O_3$–liquid metal systems (——).

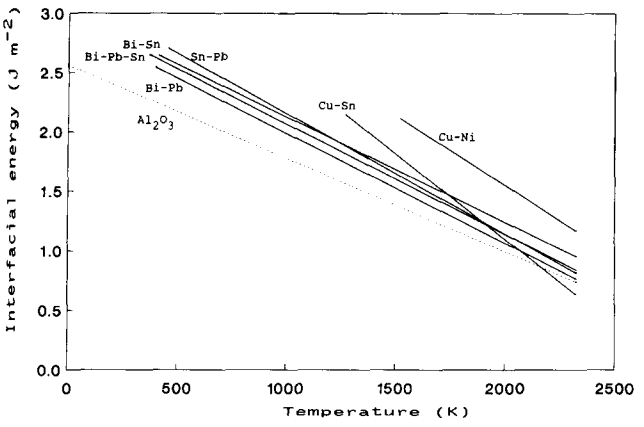


**Fig. 7.** Temperature dependence of the surface energy ($\gamma_{SV}$) of $Al_2O_3$ (– – –) and of the interfacial energy ($\gamma_{SL}$) in $Al_2O_3$–liquid alloy systems (——).

(dashed line) covers the temperature range from 0 to 2323 K.

It is observed in Figs 6 and 7 that at high temperatures the lines of some liquid metals and alloys cross the surface energy line of alumina. Obviously the crossing point separates the non-wetting ($\gamma_{SL} > \gamma_{SV}$ and $\theta > 90°$) from the wetting situation ($\gamma_{SL} < \gamma_{SV}$ and $\theta < 90°$). This observation leads to the conclusion that in some systems good bonding at the ceramic–metal interface could be achieved at high temperatures, i.e. wetting situation.

In the literature only one reference concerning experimental results for the $Al_2O_3$–Ni system appears, given by Kingery.[26] In this paper the interfacial energy of $Al_2O_3$–Ni was determined by the multiphase equilibrium method, and is given as 1·860 J m$^{-2}$ at 2123 K. This value deviates substantially from the value calculated by the linear temperature function in Table 7, 1·332 J m$^{-2}$. This deviation is due to the difference of the contact angle values at this temperature.

Other values of interfacial energies reported in the open literature for the $Al_2O_3$–liquid metal systems have been obtained from contact angle measurements. In all these papers the surface energy, $\gamma_{SV}$, of $Al_2O_3$ used for the calculations (eqn (2)) is taken to be 0·905 J m$^{-2}$ at 2123 K as determined by Kingery.[26] The required surface energy is obtained by extrapolation from this value to the investigated temperature with a temperature coefficient of $-0{\cdot}1 \times 10^{-3}$ J m$^{-2}$ K$^{-1}$ for ionic-bonded materials. However, this type of extrapolation leads to substantial deviations for the interfacial energies between the literature data and the data of Tables 7 and 8, especially in low melting point metal or alloy systems.

The influence of the temperature coefficient becomes weaker at high temperatures. Therefore, a better agreement with experimental data is observed. The literature values of the interfacial energies given as 2·2 J m$^{-2}$ at 1423 K in $Al_2O_3$–Cu,[27] 2·075 J m$^{-2}$ at 1823 K in $Al_2O_3$–Ni[28] and 2·097 J m$^{-2}$ at 1873 K in $Al_2O_3$–Co[28] are in good agreement with the values obtained from temperature functions of Table 7, i.e. 2·385, 1·916 and 2·221 J m$^{-2}$, respectively.

As shown in Table 7, the values of the interfacial energies in $Al_2O_3$–liquid metal systems at the metal's melting point are limited within a short range (2·35–2·75 J m$^{-2}$). However, this is not the case for nickel, possibly due to the formation of a new phase, and palladium, where the type of the interfacial bond is uncertain.[29] This observation leads to the conclusion that a reasonable approach to the wettability in such systems at the melting point of the metals may be obtained by just using an average interfacial energy value between alumina and liquid metals. This approach seems to be independent of the type of metal and applies, in particular, to those metals with high melting point.

The non-system-specific average value of interfacial energy at the melting point of the metals described in the previous paragraph can be further refined to become system-specific with the calculation method now proposed.

Good & Girifalco[30] showed that interfacial energy between the solid and liquid phases is given by

$$\gamma_{SL} = \gamma_{SV} + \gamma_{LV} - 2\phi(\gamma_{SV}\gamma_{LV})^{1/2} \qquad (10)$$

where $\phi$ is a magnitude characteristic of the system which depends on the molar volumes of the phases in contact. It appears from eqn (10) that $\gamma_{SL}$ depends on geometric mean of surface interactions, $(\gamma_{SV}\gamma_{LV})^{1/2}$, as well as on the molar volumes.

However, on the basis of the present analysis and experimental results the conclusion was reached that $\gamma_{SL}$ should not only depend on a gross description of the molar volumes but also on the geometric details of the surface determined by the site of the oxide ions as well as the stoichiometry of the elements in the oxide. Accordingly, the following empirical relation is proposed:

$$\gamma_{SL} = \left(K\frac{V_{Metal}}{V_{Oxide}} + 1\right)^{2/3}(\gamma_{SV}\gamma_{LV})^{1/2} \qquad (11)$$

where $V_{Metal}$ and $V_{Oxide}$ are the molar volumes of the metal and the oxide, respectively. The constant $K$ is the ratio of ion radii in the oxide, $R_{Oxygen}/R_{Metal}$, multiplied by the ratio of the stoichiometry of the elements, i.e. in $Al_2O_3$ $K = 3R_O/2R_{Al} = 4{\cdot}2$. For the calculations in $Al_2O_3$–liquid metal systems, the

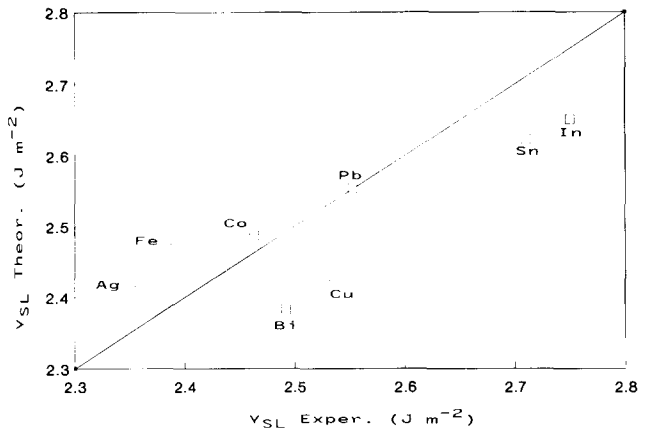


**Fig. 8.** Plot demonstrates correlation between interfacial energy ($\gamma_{SL}$) values determined by experiments and those determined by the empirical eqn (10) in $Al_2O_3$–liquid metal systems.

values of $\gamma_{SV}$ and $\gamma_{LV}$ were obtained from eqn (9) and Table 3, respectively. The molar volume of the metals, $V_{Metal}$, is calculated using the density values at their melting points.[15] The molar volume of the alumina, $V_{Oxide}$, is determined at the melting points of the metals using the following values: density, $\rho = 3{\cdot}97\ Mg\ m^{-3}$ at 293 K; linear expansion coefficients, $7{\cdot}6 \times 10^{-6}\ K^{-1}$ at 293–773 K, $8{\cdot}6 \times 10^{-6}\ K^{-1}$ at 773–1273 K and $9{\cdot}6 \times 10^{-6}\ K^{-1}$ at 1273–1773 K.[31]

Figure 8 shows the experimental and the predicted values, using eqn (11), of the interfacial energies in $Al_2O_3$–liquid metal systems. A good agreement is observed between the predicted and experimental values at the melting point of the non-reactive metals.

At present similar experiments and analyses are being performed in other oxide–liquid metal systems and similar results have been obtained.

## 5 Conclusions

(1) The contact angles in $Al_2O_3$–liquid metal and $Al_2O_3$–liquid alloy systems were determined experimentally. It was found that the metals and the alloys examined, in the investigated temperature range, do not wet the polycrystalline alumina.

(2) Using the relation of simple liquid mixtures, the temperature dependence of the surface energies of liquid alloys was calculated.

(3) The values of the work of adhesion in $Al_2O_3$–liquid metal and alloy systems increase when the temperature as well as the melting point of the metal or the alloy increases. For non-reactive $Al_2O_3$–liquid metal systems the interactions at the interface can be explained by a chemical bond establishment, particularly in the case of transition metals.

(4) The linear temperature functions of the interfacial energies in $Al_2O_3$–liquid metal and alloy systems were obtained assuming that the influence of metal vapors on the surface energy of $Al_2O_3$ can be neglected. The values of the interfacial energies at the melting point of the metals in non-reactive $Al_2O_3$–liquid metal systems vary within a restricted region (2·35–2·75 J m$^{-2}$).

(5) The proposed empirical relation permits the calculation of the interfacial energy at the melting point of the metals for non-reactive $Al_2O_3$–liquid metal systems. A good agreement between predicted and experimental values was observed.

## Acknowledgements

The present work was performed in the framework of the EUREKA (EU-294) Project and is financially supported by the Greek Ministry for Industry, Energy and Technology.

## References

1. Thummler, F. J., *Eur. Ceram. Soc.*, **6** (1990) 139–51.
2. Nicholas, M. G., In *Designing Interfaces for Technological Applications*, ed. S. D. Peteves. Elsevier Applied Science Publishers, London, 1989, pp. 49–76.
3. Nikolopoulos, P., *J. Mater. Sci.*, **20** (1985) 3993–4000.
4. Angelopoulos, G., Jauch, U. & Nikolopoulos, P., *Mat.-Wiss. Werkstofftech.*, **19** (1988) 168–72.
5. Halden, F. A. & Kingery, W. D., *J. Phys. Chem.*, **59** (1955) 557–9.
6. Nikolopoulos, P. & Schulz, B., *J. Nucl. Mater.*, **82** (1979) 172–8.
7. Bashford, F. & Adams, S. C., *An Attempt to Test the Theories of Capillary Action*. University Press, Cambridge, 1883, p. 63.
8. Nikolopoulos, P., Nazare, S. & Thummler, F., *J. Nucl. Mater.*, **71** (1977) 89–94.
9. Chatain, D., Rivollet, I. & Eustathopoulos, N., *J. Chim. Phys.*, **83** (1986) 561–7.
10. Zagar, L. & Bernhardt, W., Forschungsberichte des Landes Nordrhein-Westfahlen. Westdeutscher Verlag, Köln, 1966, No. 1733.
11. Naidich, J. V., In *Progress in Surface and Membrane Science*, Vol. 14, ed. D. A. Cadenhead & J. F. Danielli. Academic Press, New York, 1981, pp. 353–484.
12. Standing, R. & Nicholas, M., *J. Mater. Sci.*, **13** (1978) 1509–14.
13. Trumble, K. P. & Ruhle, M., *Z. Metallkunde*, **81** (1990) 749–55.
14. Lang, G., *Z. Metallkunde*, **67** (1976) 549–58.
15. Allen, B. C., In *Liquid Metals*, ed. S. Z. Beer. Marcel Dekker, New York, 1972, pp. 161–212.

16. Lang, G., Laty, P., Joud, J. C. & Desre, P., *Z. Metallkunde*, **68** (1977) 113–16.
17. Miedema, A. R. & Boom, R., *Z. Metallkunde*, **69** (1978) 183–90.
18. Belton, J. W. & Evans, M. G., *Trans. Faraday Soc.*, **41** (1945) 1–12.
19. Guggenheim, E. A., *Trans. Faraday Soc.*, **41** (1945) 150–6.
20. Hoar, T. P. & Melford, D. A., *Trans. Faraday Soc.*, **53** (1957) 315–26.
21. Yeum, K. S., Speiser, R. & Poirier, D. R., *Metall. Trans. B*, **20B** (1989) 693–703.
22. Li, J. G., Goudurier, L. & Eustathopoulos, N., *J. Mater. Sci.*, **24** (1989) 1109–16.
23. Monma, K. & Suto, H., *Trans. Japan Inst. Met.*, **2** (1960) 143–7.
24. Sotiropoulou, D., Surface and interfacial properties of stabilized zirconia in contact with liquid metals. PhD thesis, Chem. Eng. Dept, University of Patras, Patras, 1990.
25. Nikolopoulos, P., Ondracek, G. & Sotiropoulou, D., *Ceram. Int.*, **15** (1989) 201–6.
26. Kingery, W. D., *J. Amer. Ceram. Soc.*, **37** (1954) 42–5.
27. Evemenko, U. N., Naidich, Yu. V. & Nosonovich, A. A., *Russ. J. Phys. Chem.*, **34** (1960) 566–8.
28. Evemenko, U. N. & Nizhenko, V. I., *Russ. J. Phys. Chem.*, **35** (1961) 638–40.
29. Klomp, J. T., In *Ceramic Microstructures '86. Role of Interfaces*, Materials Science Research, Vol. 21, ed. J. A. Pask & A. G. Evans. Plenum Press, New York, 1987, pp. 307–18.
30. Good, R. J. & Girifalco, L. A., *J. Phys. Chem.*, **64** (1960) 561–5.
31. Lynch, J. F., Ruderer, C. G. & Duckworth, W. H., *Engineering Properties of Selected Ceramic Materials*. The American Ceramic Society, Columbus, OH, 1966, pp. 5.4.1–6.